THE JOURNAL OF BIOLOGICAL CHEMISTRY VOL. 287, NO. 50, pp. 42138–42149, December 7, 2012
© 2012 by The American Society for Biochemistry and Molecular Biology, Inc. Published in the U.S.A.

Self-cleavage of Human CLCA1 Protein by a Novel Internal Metalloprotease Domain Controls Calcium-activated Chloride Channel Activation*[S]◆

Received for publication, August 13, 2012, and in revised form, October 29, 2012 Published, JBC Papers in Press, October 30, 2012, DOI 10.1074/jbc.M112.410282

Zeynep Yurtsever[‡§1], Monica Sala-Rabanal[¶‖1], David T. Randolph[§], Suzanne M. Scheaffer[§], William T. Roswit[§], Yael G. Alevy[§], Anand C. Patel[**‡‡], Richard F. Heier[§], Arthur G. Romero[§**], Colin G. Nichols[¶‖], Michael J. Holtzman[§¶**], and Tom J. Brett[§¶**§§2]**

*From the [‡]Biochemistry Program, Departments of [§]Internal Medicine and [¶]Cell Biology and Physiology, [‖]Center for Investigation of Membrane Excitability Diseases, **Drug Discovery Program, [‡‡]Department of Pediatrics, and [§§]Department of Biochemistry and Molecular Biophysics, Washington University School of Medicine, St. Louis, Missouri 63110*

Background: CLCA proteins activate CaCCs; CLCAs have roles in cancer and inflammatory lung diseases, but their mechanism of action is unknown.
Results: CLCA proteins must undergo self-cleavage via their own novel metalloprotease domain in the N terminus to activate CaCCs.
Conclusion: Self-cleavage unmasks the N-terminal fragment, which alone activates CaCCs.
Significance: This work identifies a unique ion channel activation mechanism defining framework to understand CLCA functions in diseases.

The chloride channel calcium-activated (CLCA) family are secreted proteins that regulate both chloride transport and mucin expression, thus controlling the production of mucus in respiratory and other systems. Accordingly, human CLCA1 is a critical mediator of hypersecretory lung diseases, such as asthma, chronic obstructive pulmonary disease, and cystic fibrosis, that manifest mucus obstruction. Despite relevance to homeostasis and disease, the mechanism of CLCA1 function remains largely undefined. We address this void by showing that CLCA proteins contain a consensus proteolytic cleavage site recognized by a novel zincin metalloprotease domain located within the N terminus of CLCA itself. CLCA1 mutations that inhibit self-cleavage prevent activation of calcium-activated chloride channel (CaCC)-mediated chloride transport. CaCC activation requires cleavage to unmask the N-terminal fragment of CLCA1, which can independently gate CaCCs. Gating of CaCCs mediated by CLCA1 does not appear to involve proteolytic cleavage of the channel because a mutant N-terminal fragment deficient in proteolytic activity is able to induce currents comparable with that of the native fragment. These data provide both a mechanistic basis for CLCA1 self-cleavage and a novel mechanism for regulation of chloride channel activity specific to the mucosal interface.

The chloride channel calcium-activated (CLCA)[3] proteins are a complex family targeted for a role in cancer (1, 2) and inflammatory diseases (3) but are poorly understood in terms of molecular structure and function. The original annotation of this family as calcium-activated chloride channels (CaCCs) was based on the observation that overexpression of several different CLCA paralogues from various species all induced chloride current in response to cytosolic calcium flux (4, 5). However, bioinformatic (3) and experimental data (6–8) indicate that CLCA proteins generally lack essential features to form ion channels by themselves as they either contain only a single transmembrane anchor or are fully released in soluble form. Indeed, a recent study provides strong evidence that human CLCA1 functions as a secreted factor that increases the activity of other proteins that act as endogenous CaCCs (9).

Significant interest in CLCA proteins stems from their association with human disease. CLCA1 has been linked to the pathogenesis of human asthma and chronic obstructive pulmonary disease; CLCA1 expression is significantly increased in the airways of these types of patients (6), and polymorphisms in the *CLCA1* gene have been reported in a subset of patients with asthma (10) and chronic obstructive pulmonary disease (11). In animal models of these diseases, the mouse and horse orthologues of CLCA1 were shown to be necessary and sufficient for driving increased mucus production (12–15). Most importantly, there is evidence that CLCA1 stimulates an increase in mucus production by initiating a MAPK signaling pathway to express mucins (the major protein component of mucus) in

* This work was supported, in whole or in part, by National Institutes of Health Grants RO1-HL073159 and P50-HL107183 (to M. J. H.) and RO1-HL54171 (to C. G. N.). This work was also supported in part by funding from the American Heart Association (Grant 0730336N) and American Cancer Society Grant IRG-58-010-52 (to T. J. B).
◆ This article was selected as a Paper of the Week.
[S] This article contains supplemental Fig. S1, a scheme, and supplemental text.
[1] Both authors contributed equally to this work.
[2] To whom correspondence should be addressed: Campus Box 8052, 660 S. Euclid, St. Louis, MO 63110. Tel.: 314-747-0018; Fax: 314-362-8987; E-mail: tbrett@wustl.edu.

[3] The abbreviations used are: CLCA, chloride channel calcium-activated; hCLCA1, human CLCA1; CaCC, calcium-activated chloride channel; CF, cystic fibrosis; CFTR, cystic fibrosis transmembrane conductance regulator; VWA domain, von Willebrand type A domain; TEV, tobacco etch virus; MMP, matrix metalloprotease; ADAM, a disintegrin and metalloproteinase; ADAMTS, a disintegrin and metalloproteinase with thrombospondin motifs; pF, picofarads.

humans, a pathway that is highly activated in humans with chronic obstructive pulmonary disease (16). Understanding the mechanism of CLCA function in signaling for mucus overproduction could lead to effective anti-mucus therapies.

Other studies suggest that CLCA proteins are also associated with the pathogenesis of cystic fibrosis (CF); mutations in the cystic fibrosis transmembrane conductance regulator (CFTR), a chloride channel found in the apical membranes of mucosal epithelial cells, disrupt normal chloride transport, resulting in insufficiently salted and hydrated mucus. Fatal intestinal disease found in CFTR-deficient mice, however, is corrected by overexpression of native mouse CLCA3 (an orthologue of human CLCA1) (17). Consistent with this observation, a mutation in the *CLCA1* gene is found in a subset of CF patients with more severe intestinal disease (18). These studies indicate that CLCA1 may function to alleviate CFTR deficiency symptoms by increasing endogenous CaCC activity and compensating for defective CFTR-mediated chloride transport. To that end, an understanding of the mechanism of activation could also be exploited to produce effective CF therapies.

In the present study, we aimed to better understand CLCA1 function with an analysis of CLCA processing. We recognized that proteolytic processing is critical to signaling function for other proteins (19) and that CLCA proteins are uniformly subjected to proteolytic cleavage within the secretory pathway to yield N- and C-terminal CLCA fragments of ~70 and 38 kDa, respectively (3). Here, using a combination of sequence analysis, structure prediction, and biochemical, biophysical, and electrophysiological techniques, we demonstrate that all CLCA proteins contain a consensus cleavage motif, which is recognized by a novel zincin metalloprotease domain located within the N terminus of CLCA itself. In addition to self-proteolysis, we also demonstrate that CLCA paralogues are capable of cross-proteolysis. Finally, we demonstrate that this self-cleavage event is a required step for CLCA1-based activation of CaCCs, which is mediated solely through the N-terminal fragment. Taken together, these data support a paradigm of CLCA activation through self-proteolysis to unmask an N-terminal fragment capable of gating CaCCs.

EXPERIMENTAL PROCEDURES

Expression Constructs—Constructs were generated using standard PCR and molecular biology techniques. All constructs were verified by DNA sequencing. For determination of proteolytic cleavage sites, full-length mature-form CLCA proteins (*i.e.* without their endogenous signal sequences) were cloned into the pHLsec vector (20) containing an optimized signal sequence and C-terminal hexahistidine tag. Soluble CLCAs were designed by omitting C-terminal membrane anchors from those CLCAs that contain them (*i.e.* human CLCA2, human CLCA4, mouse CLCA4). Specifically, constructs contained the following residues: CLCA1 22–914; CLCA2 32–899; CLCA4 22–876; mouse CLCA3 22–913; mouse CLCA4 22–897. Mutations were introduced into the full-length CLCA1 pHLsec construct using Phusion mutagenesis (New England Biolabs) for mutational analysis of the cleavage site and predicted active site residues. Full-length CLCA1 and select mutants containing the optimized signal sequences were subcloned from pHLsec constructs into the pCDNA3.1 expression vector (Invitrogen). A dual-tagged CLCA1 construct in pCDNA3.1 was made by inserting a FLAG tag directly after the signal sequence and a hexahistidine tag at the C terminus of the protein. Mammalian cell expression constructs encompassing the protease and VWA domain of CLCA1 (22–477), CLCA2 (32–455), and CLCA4 (22–459) as well as the substrate region (285–915) of CLCA1 were cloned into pHLsec with C-terminal hexahistidine tags. A tag-free bacterial expression construct composed of the protease and VWA domain of CLCA1 (22–477) was cloned into pET23b. Mammalian expression constructs of CLCA1 N-terminal fragment (22–695) and C-terminal fragment (696–915) were cloned into the pHLsec vector containing an optimized signal sequence and C-terminal hexahistidine tag (20).

Protein Expression and Purification—Proteins in mammalian expression vectors were expressed by transient transfection of FreeStyle 293F cells using 293Fectin cultured in serum-free FreeStyle 293 media (Invitrogen). Culture supernatants were collected 72 h after transfection, and proteins were purified to homogeneity using nickel affinity chromatography. CLCA1 22–477 was expressed in *Escherichia coli* as insoluble protein that was recovered from inclusion bodies, denatured in 6 M guanidine hydrochloride, and refolded by rapid dilution into buffer consisting of 50 mM Tris, pH 8.5, 400 mM arginine, 5 mM reduced glutathione, 0.5 mM oxidized glutathione, 10 mM $CaCl_2$, 0.1 mM $ZnCl_2$. The resulting soluble protein was purified by gel filtration followed by ion exchange chromatography. The protein was well folded as assessed by circular dichroism.

Determination of Proteolytic Cleavage Sites by Edman Degradation—Full-length CLCA proteins were expressed by transient transfection of FreeStyle 293F cells as described above. Culture supernatants were collected 72 h after transfection, and C-terminal fragments were captured and purified using nickel affinity chromatography. C-terminal fragments were isolated by SDS-PAGE and membrane transfer and then analyzed by N-terminal sequencing (Edman degradation) to determine the site of proteolytic cleavage. The first 5 residues were identified in each case. Additionally, intracellular processing of CLCA1 was assessed by immunoprecipitating the C-terminal fragment from the lysates of washed lung epithelial H292 cells transfected with a CLCA1-expressing adenovirus. Isolation and analysis were performed as described above.

Sequence Analysis—CLCA sequences and naming were based on recent nomenclature as recently reviewed (3).

Analysis of Proteolytic Processing of Wild-type and Mutant CLCA1—Mutants were expressed in 293F cells as described above. Culture supernatants and cell lysates were collected 72 h after transfection and analyzed by Western blot using antibodies that recognize either the N-terminal fragment (anti-N-CLCA1 mAb 8D3; epitope region: 477–695) or the C-terminal fragment (anti-His_6 antibody, Bethyl Laboratories). Processing of the dual-tagged hCLCA1 construct was analyzed using anti-FLAG antibody (M2 mAb, Sigma) in addition to the other antibodies. To test the CLCA1 tobacco etch virus (TEV) mutant for cleavage by exogenously added TEV protease, transfection was carried out as above followed by the addition of TEV protease to the culture medium (to a concentration of 0.2 mg/ml) 48 h after

transfection. Samples were collected after 72 h after transfection and analyzed as above.

Proteolytic Digestion Assays—Purified protease (CLCA1 22–477, CLCA2 32–455, and CLCA4 22–459) and substrate (CLCA1 285–915) were produced as described above. Digestion experiments were carried out by incubating substrate (0.5 μM) and protease (2.0 μM) in 100 μl of digestion buffer (20 mM Hepes, pH 7.5, 150 mM NaCl, 10 mM $CaCl_2$, 10 μM $ZnCl_2$) at 37 °C for 18 h with samples taken at discrete time points and analyzed by SDS-PAGE/Western blot using the anti-CLCA1 mAb 8D3. Digestion experiments in the presence of inhibitors were carried out with GM-6001 (Millipore), Marimastat (Tocris), Batimastat (Tocris), or Zeynepstat001 at 40 μM or Halt (Thermo) at 1× concentration. All inhibitor stocks were dissolved in dimethyl sulfoxide (DMSO).

Fluorogenic CLCA1 Peptide Digestion Assays—A fluorogenic peptide substrate consisting of a donor-acceptor FRET pair conjugated to the human CLCA1 cleavage sequence was synthesized by AnaSpec (DABCYL-QQSGALYIPG-EDANS). Experiments were carried out at 37 °C in the digestion buffer described above. Reaction progress was monitored using a BioTek plate fluorometer (excitation, 340 nm; emission, 490 nm). Refolded CLCA1 (22–477) was used as the protease. For reactions in the presence of inhibitors, [protease] = 10 μM, [substrate] = 3.25 μM, and [inhibitor] = 20 or 40 μM, respectively. Experiments were conducted in triplicate.

Chemical Synthesis of a Custom MMP Inhibitor—Synthesis of Zeynepstat001 is described in the supplemental material.

Heterologous Expression for Electrophysiology—Mutations predicted to interfere with the metalloprotease activity of CLCA1 (H156A, E157Q) or a disrupted cleavage site (contra) were generated using the pCDNA3.1 expression vector; cDNAs encoding the N-terminal or C-terminal fragments of CLCA1 were cloned into pHLsec, as described above. HEK293T cells were plated in 6-well dishes and cultured in Dulbecco's modified Eagle's medium (Invitrogen) supplemented with 10% fetal bovine serum, 10^5 units/liter penicillin, and 100 mg/liter streptomycin. At 80% confluency, cells were transfected with the relevant plasmids using 293Fectin transfection reagent at a 1 μg of DNA to 2 μl of 293Fectin ratio, and the amount of DNA per well was kept constant at 2 μg. For identification of expressing cells, 1% of EGFP-pCDNA3.1 plasmid was added to all transfection mixtures. 24 h after transfection, cells were trypsinized and replated at low density on glass coverslips. Expression of wild-type (WT), mutant, and fragment proteins was confirmed by Western blot of culture supernatants 48 h after transfection, as described above.

Whole-cell Patch Clamp Recordings—Experiments were performed at 25 °C, 48–72 h after transfection. Cells that fluoresced under ultraviolet light were selected for analysis. Micropipettes were prepared from nonheparinized hematocrit glass (Kimble-Chase) on a horizontal puller (Sutter Instrument) and filled to a typical electrode resistance of 2 megaohms with pipette solution containing 126 mM choline chloride, 10 mM Hepes and 10 mM EGTA, in the absence or presence of 9.95 mM $CaCl_2$ to attain 10 μM free Ca^{2+}, as calculated by means of the CaBuf program (available through KU Leuven). The standard extracellular solution contained 126 mM NaCl, 10 mM Hepes, 30 mM sucrose, 2 mM $CaCl_2$, and 2 mM $MgCl_2$. To determine the background currents, the cells were superfused with a Cl^--free solution containing 126 mM Na^+ gluconate, 10 mM Hepes, 10.5 mM sucrose, 7 mM Ca^{2+} gluconate, and 3.5 mM Mg^{2+} gluconate. The pH of all solutions was adjusted to 7.4 with Tris. After formation of a gigaohm seal and establishment of whole-cell configuration, cells were voltage-clamped at −80 mV. A pulse protocol was applied in which membrane potential (V_m) was held at −80 mV for 500 ms and stepped to a test value for 1000 ms before returning to the holding potential for an additional 500 ms. The test potential varied from −100 to +80 mV in 20 mV increments. Currents were measured at the end of the 1000-ms voltage pulse. Membrane capacitance was calculated from the integral of the current transient in response to 10-mV depolarizing pulses and was monitored for stability throughout the experiment. Data were filtered at 2 kHz, and signals were digitized at 5 kHz with a Digidata 1322A (Molecular Devices). Axoscope and pClamp software (Molecular Devices) were used for pulse protocol application and data acquisition. Data were analyzed using Clampfit (version 10.1, Molecular Devices) and Excel (Microsoft). SigmaPlot 10.0 (Systat Software) and CorelDRAW X3 13.0 (Corel Corp.) were used for statistics and figure preparation. Results are presented as mean ± S.E., and unpaired Student's *t* test was used to evaluate statistical differences between groups.

RESULTS

CLCA Proteins Share a Common Cleavage Site—Proteolytic processing plays a central role in almost all biological networks, and dysregulation is implicated in a broad range of diseases (19). With this in mind, we sought to investigate the role of proteolytic processing in CLCA protein function. Mammals express 4–8 CLCA family members, predominantly at mucosal surfaces. All CLCAs have been observed to undergo proteolytic processing when expressed in mammalian cells; the protein gets cleaved into two fragments of ~70 kDa of the N terminus and 38 kDa of the C terminus (3). We reasoned that elucidation of the cleavage site might allow for identification of the protease responsible for this activity. To facilitate this analysis, we generated tagged soluble expression constructs of the three human CLCA proteins (CLCA1, CLCA2, and CLCA4), as well as two mouse CLCAs (CLCA3 and CLCA4), and expressed each of them in mammalian cells (Fig. 1*A*). Cleavage sites were determined by amino-terminal sequencing of secreted C-terminal fragments from media supernatants. All five of the CLCA proteins were cleaved at a common site (Fig. 1*B*). Because our data and previous studies indicated that CLCA proteins are processed intracellularly (7, 8, 21, 22), we also analyzed CLCA1 retrieved from cell lysates to investigate the possibility of sequential processing. This sample displayed the same cleavage site as the fully secreted proteins found in supernatants. Analysis of all known CLCA sequences from higher mammals reveals a high degree of conservation in this region (Fig. 1*B*), consistent with a consensus cleavage sequence shared among CLCA family proteins (Fig. 1*C*) and a common protease, or family of proteases, responsible for CLCA cleavage.

To verify the location of the cleavage site, we tested the effect of mutations to the experimentally determined cleavage site

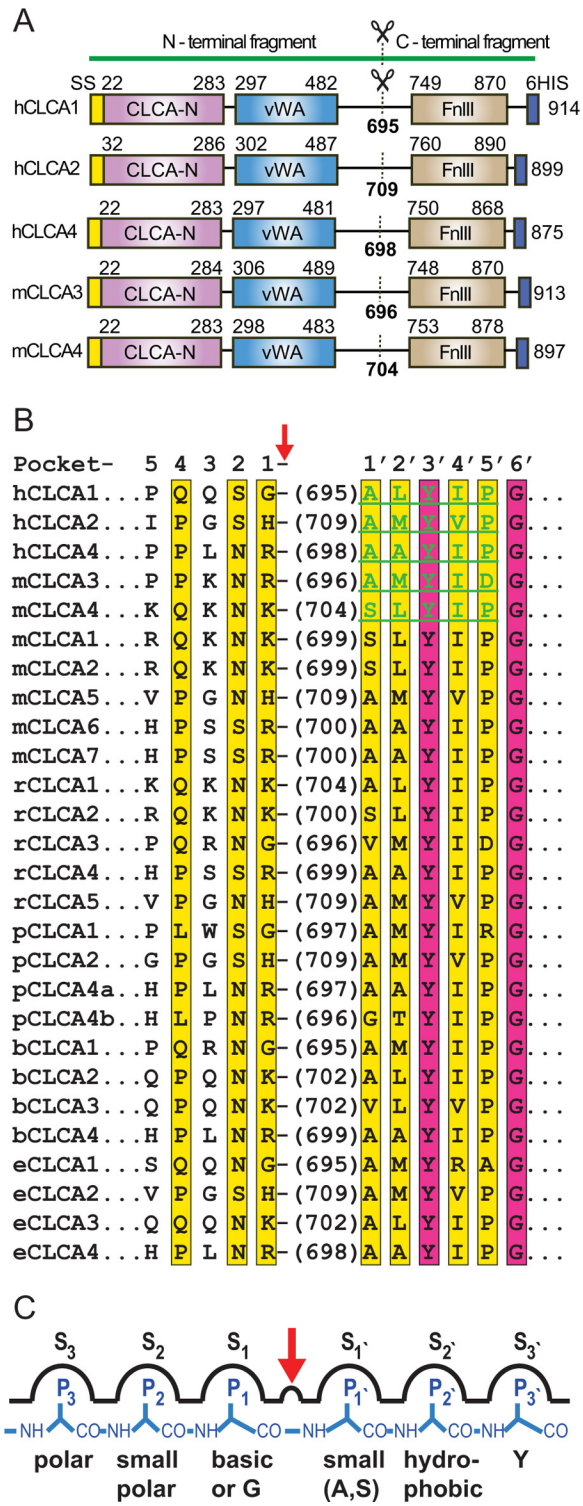

FIGURE 1. **Identification of a consensus cleavage site in CLCA proteins.** *A*, schematic of soluble CLCA constructs used to experimentally determine proteolytic cleavage sites. *Dashed line* denotes cleavage site with scissile bond residue number listed underneath. Labels denote the following: *SS*, signal sequence; *CLCA-N*, N-terminal CLCA domain; *FnIII*, fibronectin type III domain; *6His*, hexahistidine tag. *B*, comparison of CLCA sequences in the region of the proteolytic cleavage site. Results of N-terminal sequencing are *underlined* and *highlighted in green text*. Sequence conservation is color-coded as follows: *magenta*, invariant residues; *yellow*, conservation score of 5 or greater as determined by ALSCRIPT (49). *Lowercase letters* preceding CLCA indicate species as follows: *h* = human, *Homo sapiens*; *m* = mouse, *Mus musculus*; *r* = rat, *Rattus norvegicus*; *p* = pig, *Sus scrofa*; *b* = cow, *Bos taurus*; *e* = horse, *Equus caballus*. *C*, schematic of the consensus cleavage site in CLCAs. *S* and *P* labels refer to protease subsite and pocket designations, respectively.

sequence on proteolytic processing of CLCA1 (Fig. 2*A*). A point mutation (A696P) or variations that matched the cleavage sequence in other CLCAs (CLCA2 and CLCA4) did not affect proteolytic cleavage of CLCA1; in contrast, variations that significantly altered the consensus sequence (contra, TEV) abolished proteolytic processing (Fig. 2*B*). These mutations did not grossly affect protein folding as all variant proteins were robustly secreted into the media supernatants. Furthermore, TEV protease added to cultures expressing the TEV CLCA1 variant, in which the TEV protease cleavage site replaced the consensus site, was not cleaved either (Fig. 2*C*), suggesting that the cleavage site is not surface-exposed to exogenous proteases and may only be accessible to the internal metalloprotease domain in the natively folded full-length protein. Taken together, these results pinpoint the location of the proteolytic cleavage site in CLCA proteins and imply that a common protease with specific access to the site is responsible for cleavage of all human CLCA proteins.

Proteolytic Processing of CLCA Requires Catalytic Residues in a Predicted Zincin Metalloprotease Domain—Extensive bioinformatic searching of the MEROPS protease database (23) using the CLCA consensus cleavage sequence did not provide any reasonable candidates for the protease responsible for cleaving CLCA family members. Thus, we decided to revisit the untested hypothesis that the N-terminal CLCA-N domain itself houses a metalloprotease domain similar to that of matrix metalloproteases (MMPs) (24). Indeed, when various CLCA-N domain sequences were submitted to the updated PHYRE2 fold prediction server (25), most predictions were high-confidence hits to zincin metalloprotease catalytic domains.

The CLCA-N domain contains 8 cysteine residues that are invariant across all family members (3). With 2 of these cysteines lying in the predicted catalytic region (amino acids 22–199) (Fig. 3*C*) and 6 in an adjacent cysteine-rich domain (amino acids 200–283) (26) (Fig. 3*A*), it is most likely that the CLCA-N domain is architecturally similar to the ADAM or ADAMTS family of zinc metalloproteases, rather than MMPs. Like the CLCA-N domain, ADAM and ADAMTS contain disulfide bonds in their catalytic regions (Fig. 3*A*) (27). The catalytic domains of zinc metalloproteases contain a common H**E***XX*H*XX*G*XX*H motif, which includes the catalytically required glutamate (bold) and zinc-chelating residues (3 histidine residues) (27). CLCA sequences in the predicted catalytic region are almost completely invariant and reveal a similar but unique catalytic motif: H**E***XX*H*XXX*G*XX*DE (Fig. 3*C*). Previous studies have reported that mutations of Glu-157 in human CLCA1 (24), murine CLCA3 (28), and murine CLCA6 (29) to Gln all produce mutant proteins that are not proteolytically processed. However, the significance of these results is difficult to interpret as these studies probed the protein from crude cell lysates. The observed lack of cleavage could have been due to loss of the catalytically required residue or to gross misfolding of the protein caused by the mutation, which would also result in detecting only full-length proteins in cell lysates. To unambiguously assess the catalytic importance of these predicted

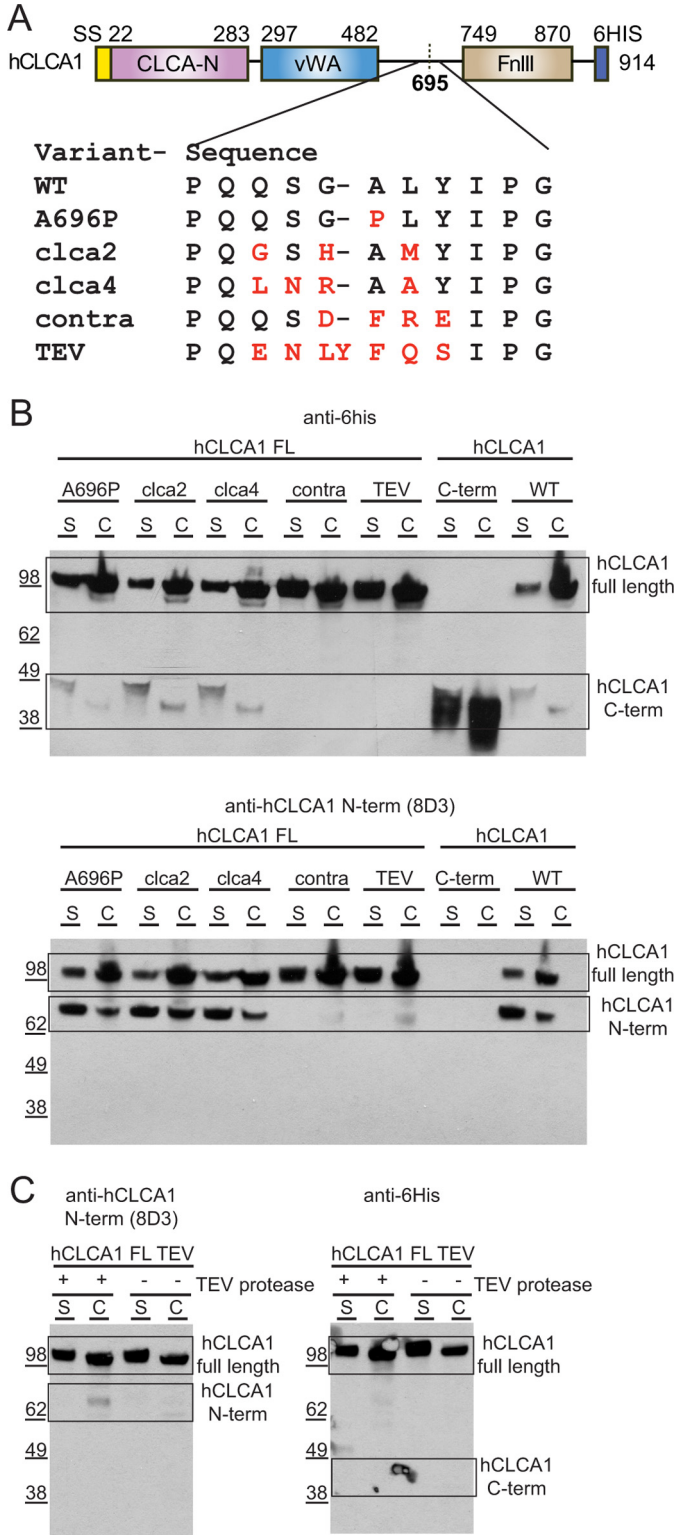

FIGURE 2. **Mutations opposing the consensus cleavage sequence prevent proteolytic processing of hCLCA1.** *A*, schematic of hCLCA1 displaying the sequence encompassing the proteolytic site. Sequences are labeled as follows: *SS*, signal sequence; *WT*, wild type sequence; *A696P*, proline mutant at the scissile bond; *clca2*, hCLCA2 cleavage site mutated into hCLCA1; *clca4*, hCLCA4 cleavage site mutated into hCLCA1; *contra*, severe mutations contrary to the CLCA consensus cleavage sequence; *TEV*, tobacco etch virus protease cleavage site mutated into hCLCA1 site; *6His*, hexahistidine tag. Mutated residues are *highlighted in red*. *B*, expression of mutant versions of hCLCA1 in HEK293T cells. Samples were taken from media supernatants (*S*) and lysed cells (*C*), separated by SDS-PAGE, and analyzed by Western blot for either hCLCA1 C terminus (*C-term*) (His$_6$ antibody, *top blot*) or hCLCA1 N terminus (*N-term*) (8D3 mAb, *bottom blot*). Conservative mutations to the cleavage site (A696P, clca2, and clca4) do not block proteolytic processing, whereas radical variations (contra, TEV) block proteolytic processing of hCLCA1. *C*, expression of hCLCA1 FL TEV mutant in the absence and presence of TEV protease in the media (0.2 mg/ml). Secreted hCLCA1 FL TEV protein in the media supernatant was analyzed by Western blot using same antibodies as in *B*.

active site residues, we analyzed proteolytic processing of CLCA1 point mutants fully secreted into media supernatants, *i.e.* proteins that have passed the cellular quality control machinery and are correctly folded. Mutations to all predicted active site residues (H156A, E157Q, H160A, D167A, E168A) produced only uncleaved, full-length proteins, whereas wild type and a mutation outside the active site (Q150A) displayed proteolytic processing (Fig. 3*B*). The data strongly suggest that the CLCA proteins contain an N-terminal zinc metalloprotease domain and that they are capable of self-cleavage.

CLCA Metalloprotease Domains Process CLCA Proteins and Are Blocked by Specific Inhibitors—To definitively confirm the self-proteolysis activity of CLCA1 by its metalloprotease domain, we devised a biochemical digestion assay utilizing purified proteins and monoclonal antibodies. This was carried out with separately expressed and purified CLCA1 protease and CLCA1 substrate proteins produced in mammalian cells (Fig. 4*A*). Substrate consisted of the full CLCA1 protein excluding the metalloprotease domain. Protease consisted of the CLCA1 metalloprotease and VWA domains as this construct was stable and robustly expressed. These proteins were mixed, incubated at 37 °C, and then analyzed at various time points for accumulation of cleavage product by Western blot with an antibody that specifically recognized an epitope found only in the substrate. Substrate alone displayed no degradation, whereas the addition of the CLCA1 protease resulted in the appearance of a cleavage product of appropriate size over time (Fig. 4*B*). The addition of the divalent metal cation chelators EDTA and 1,10-phenanthroline completely abrogated proteolytic activity as they sequester the catalytically required zinc. In contrast, the addition of a commercial mixture containing protease inhibitors to all classes except metalloproteases (Halt, Thermo) had no effect on proteolysis of the substrate. Taken together with the previously presented mutational analysis, these data unambiguously demonstrate that the CLCA proteins contain an N-terminal metalloprotease domain responsible for self-cleavage.

We next assessed the ability of various commercial and custom MMP inhibitors to block proteolysis in this assay (Fig. 4*C*). These molecules belong to the class of hydroxamate-based inhibitors, which consist of the moiety attached to a peptide mimetic chain. These inhibitors act by chelating the zinc through the hydroxamate group with the peptide mimicking side chains binding to the S1′ and S2′ pockets (supplemental Fig. S1) (30). The inhibitors displayed differing levels of potency, with Batimastat being most effective, followed by GM-6001 and Marimastat. In addition, we synthesized a custom inhibitor consisting of a hydroxamate moiety fused to the P1′ and P2′ residues of the CLCA1 cleavage sequence (termed Zeynepstat001). This inhibitor was also effective in reducing the activity of the CLCA1 protease.

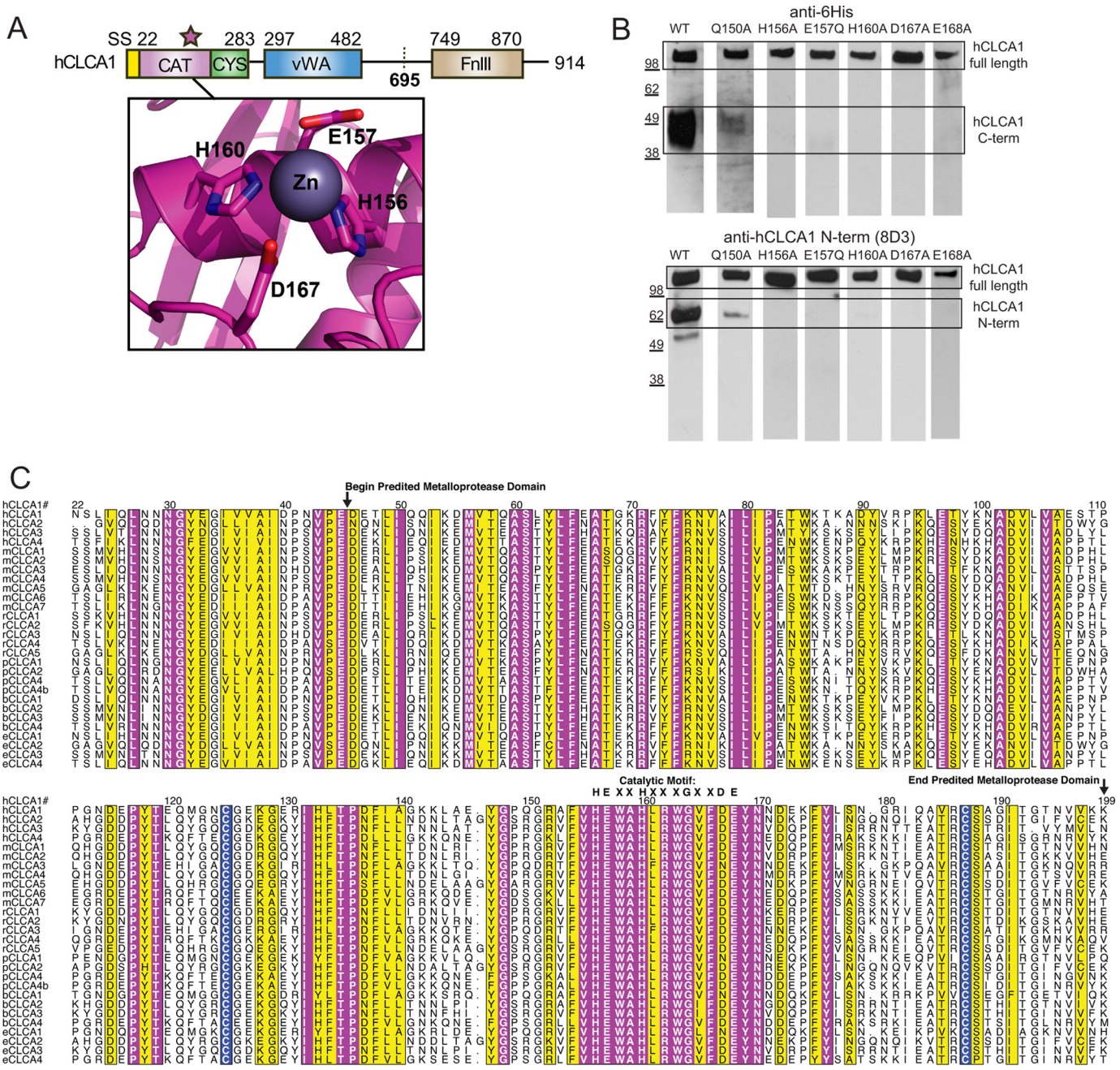

FIGURE 3. **Mutation of predicted catalytic residues blocks proteolytic processing of hCLCA1.** *A*, schematic of hCLCA1 highlighting the revised view of the CLCA-N domain as a metalloprotease. Labels denote the following: *SS*, signal sequence; *CAT*, metalloprotease catalytic domain; *CYS*, Cys-rich domain. *Inset* displays the predicted catalytic site of hCLCA1 threaded onto the structure of ADAMTS-1 (Protein Data Bank (PDB) ID: 2V4B) (50). Catalytic and zinc-chelating residues are *highlighted*. *B*, Western blot analysis of media supernatants from 293F cells expressing hCLCA1 variants. Blot was developed with a His_6 antibody (*anti-6His*), which recognizes full-length and hCLCA1 C-terminal fragment. *C*, sequence alignment of CLCA family members in the region of the catalytic site. Color coding is as follows: *magenta*, invariant residues; *yellow*, conservation score of 5 or greater as determined by ALSCRIPT (49).

Biophysical Characterization of CLCA Protease Activity—We then developed a quantitative biophysical assay to characterize CLCA1 metalloprotease activity. This assay employed a fluorogenic peptide consisting of the CLCA1 cleavage sequence conjugated to a donor-quencher FRET pair for the substrate and CLCA1 protease refolded from bacterially expressed inclusion bodies. This allowed determination of the kinetics of protease activity ($K_m = 1.10 \times 10^{-6}$ M, $V_{max} = 0.403$ fluorescence units/s) (Fig. 4, *D* and E). To further address metal dependence, experiments in the presence of chelators or excess divalent metal ions were carried out. The addition of EDTA abolished protease activity, whereas the addition of excess Zn^{2+} partially restored activity (Fig. 4*D*). In contrast, the addition of Ca^{2+} did not restore activity (data not shown). We used this assay to perform a more quantitative assessment of the MMP inhibitors. These experiments indicated that Batimastat was most effective, almost completely inhibiting protease activity at high concentrations, followed by GM-6001, Zeynepstat001, and Marimastat (Fig. 4*F*). We also tested the inhibitory activity of acetohydroxamic acid, which consists of only the zinc-binding moiety found in this class

of inhibitors. It displayed weak inhibitory activity (data not shown). Taken together, the data definitively show that CLCA1 is a Zn^{2+}-dependent metalloprotease and that inhibitors of CLCA1 protease activity can be rationally designed.

CLCA Proteases Can Cross-cleave CLCA Substrates—As multiple CLCA proteins are expressed at mucosal surfaces (3), we examined the ability of other CLCA proteases to process CLCA1 substrate. The CLCA1 substrate was incubated with

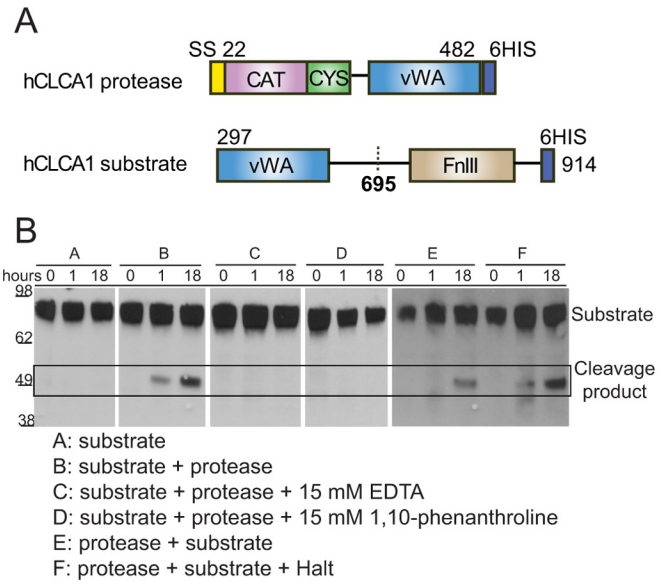

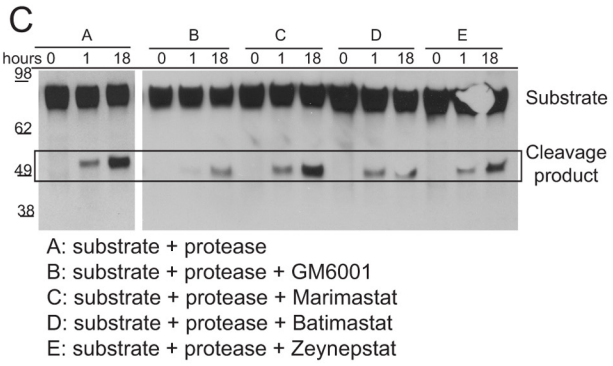

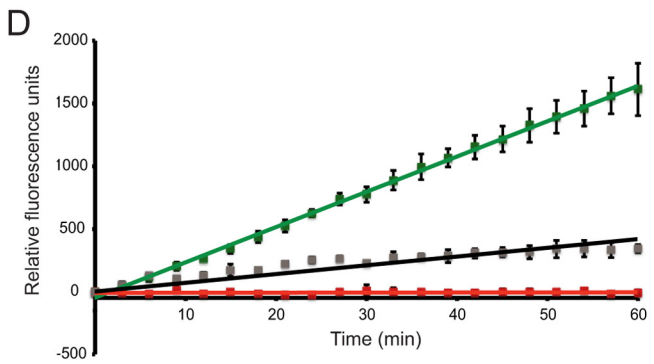

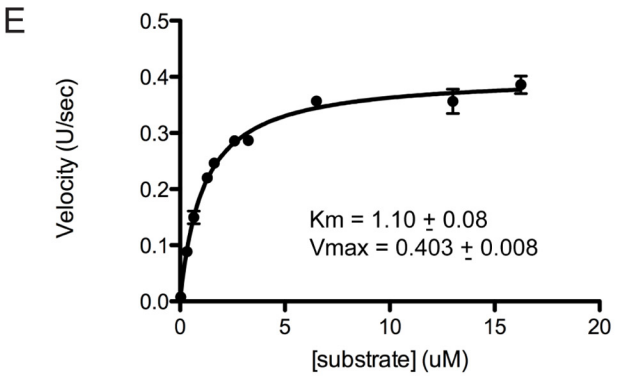

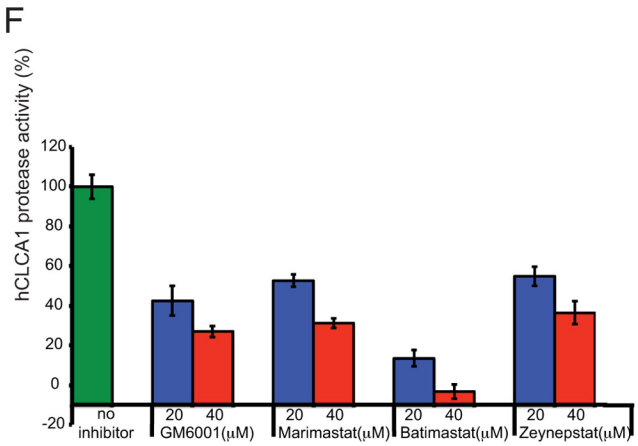

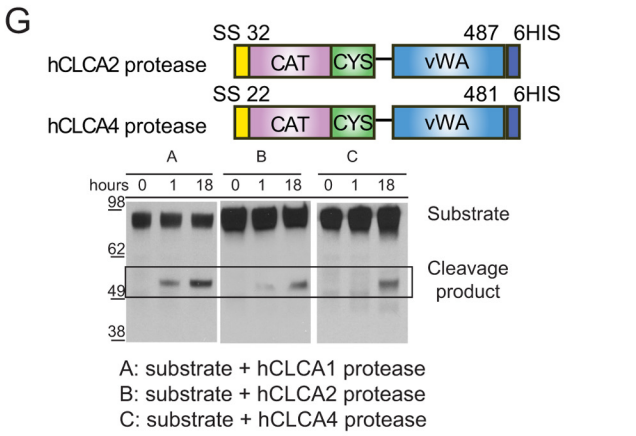

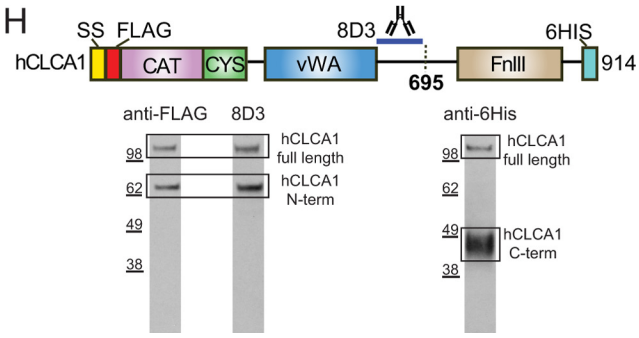

proteases, from either CLCA2 or CLCA4. Both proteases cleaved the CLCA1 substrate, although at a reduced rate (Fig. 4*G*). Taken together with the data demonstrating that self-cleavage of CLCA1 is observed in variants where the cleavage sequence is mutated to that of CLCA2 or CLCA4 (Fig. 2*B*), this result suggests that the members of the CLCA family are capable of self-cleavage as well as cross-cleavage of other family members. As multiple CLCA proteins are expressed in the same tissues, this suggests that CLCA proteins might cross-cleave each other *in vivo*; however, the physiological relevance is unknown at this time.

CLCA Proteases Do Not Contain N-terminal Prodomains—A key aspect of zincin metalloproteases is their intrinsic capacity for self-regulation, and the most common mode of regulation is removal of a prodomain. For example, MMPs and ADAM family proteases both contain an N-terminal prodomain, consisting of about 80 amino acids at the N terminus of the protein, that blocks access to the protease active site. This domain must be proteolytically removed for substrate access (27, 31). Structure predictions of the CLCA-N domain metalloprotease region indicate that the characteristic catalytic fold would begin around residue 45, which would leave a short stretch of ~20 amino acids that may act as a prodomain. To probe whether CLCA1 contains an N-terminal prodomain that regulates self-cleavage, we examined the processing of a dual-tagged hCLCA1 construct (Fig. 4*H*). This construct contains a FLAG tag directly after the signal sequence so that detection of the FLAG tag on the fully processed protein would preclude cleavage of any N-terminal prodomain. The secreted CLCA1 protein was processed normally as detected by antibodies that recognized the CLCA1 N-terminal and C-terminal fragments. In addition, Western blotting for the FLAG tag revealed an intact N terminus. Collectively, these observations indicate that CLCA1, and by implication CLCA proteins in general, do not contain N-terminal prodomains.

Self-cleavage of CLCA1 Is Required to Modulate CaCC Currents—To assess the functional role of CLCA1 self-cleavage in regulating CaCC activity, we designed mutations that generate either an inactive metalloprotease catalytic site (H156A and E157Q) or an impaired cleavage site (contra) (Fig. 5*A*) and tested their impact on CaCC currents in HEK293T cells by means of whole-cell patch clamp electrophysiology. In the presence of 10 μM intracellular Ca^{2+} and physiological concentrations of extracellular Cl^-, we observed activation of robust, slightly outward rectifying currents in HEK293T cells transfected with full-length WT CLCA1 that reversed at ~0 mV and were significantly reduced by replacement of extracellular Cl^- with gluconate (Fig. 5*C*). At +80 mV, Cl^- current density, calculated as the difference between current density in the presence (total) and absence (background) of extracellular Cl^-, was 31 ± 3 pA/pF in WT cells; individual measurements varied from 8 to 80 pA/pF but were at least 10-fold larger than in cells transfected with empty pCDNA3.1 vector (2.5 ± 0.5 pA/pF; Fig. 5*D*). When no Ca^{2+} was added to the pipette buffer, Cl^- current density was 2.7 ± 1.5 pA/pF in vector-transfected cells and 3.5 ± 1.2 pA/pF in cells transfected with WT-hCLCA1 ($n = 6$ cells each) (Fig. 5*C*). These data are in agreement with reported biophysical properties of Ca^{2+}-activated Cl^- channels in native cells and heterologous expression systems (4, 32–35) and are consistent with a previous report that CLCA1 modulates the activity of endogenous CaCCs in HEK293T cells (9). In cells transfected with CLCA1 variants, in which the metalloprotease activity was abolished (H156A, E157Q) or in which the cleavage site was disrupted (contra), the gluconate-sensitive currents were markedly decreased (Fig. 5*C*), and on average, the density of Cl^- currents was comparable with that measured in vector-transfected cells (Fig. 5*D*). Expression levels of all the variants were similar to the WT (Fig. 5*B*), indicating that the observed effects were due to impaired proteolytic processing, rather than altered synthesis, trafficking, or secretion. These data demonstrate that self-processing of CLCA1 by its novel zincin metalloprotease domain is required for its activation of CaCCs.

The N-terminal Fragment of CLCA1 Is Sufficient to Modulate CaCC Currents—To further delineate the role of CLCA self-cleavage in activation of CaCCs, we assessed the ability of each of the cleavage fragments to induce Ca^{2+}-activated currents (Fig. 5*E*). At +80 mV, Cl^- current density was 4.0 ± 0.7 pA/pF in cells transfected with empty pHLsec vector and increased to 35 ± 5 pA/pF in cells expressing full-length CLCA1. Current density in cells expressing the CLCA1 C terminus was as low as in cells transfected with empty pHLsec (4.7 ± 0.6 pA/pF). In contrast, in cells expressing the N-terminal fragment, currents were similar to those measured in cells transfected with the full-length construct (32 ± 5 pA/pF). These results demonstrate that the N-terminal fragment of CLCA1 is necessary and sufficient to regulate Ca^{2+}-activated Cl^- currents and that self-cleavage is required to release an inhibitory C-terminal frag-

FIGURE 4. **Self-cleavage of hCLCA1.** *A*, schematic of protein constructs used in purified protein proteolysis assays. Labels denote the following: *SS*, signal sequence; *CAT*, metalloprotease catalytic domain; *CYS*, Cys-rich domain; *6His*, hexahistidine tag. *B*, proteolysis of hCLCA1 substrate by hCLCA1 protease. Samples were incubated at 37 °C with samples taken at time points as noted. Reactions are labeled as follows: *A*, substrate only; *B*, substrate (0.5 μM) + protease (2 μM); *C*, substrate + protease + 15 mM EDTA; *D*, substrate + protease + 15 mM 1,10 phenanthroline; *E*, protease + substrate; *F*, protease + substrate + HALT (1×). *C*, effect of commercial and custom MMP inhibitors on hCLCA1 proteolytic cleavage. Conditions were the same as the above with the following inhibitors added to digestion reactions (at 40 μM): *B*, GM-6001; *C*, Marimastat; *D*, Batimastat; *E*, Zeynepstat. *D*, activity of purified refolded hCLCA1 protease on a fluorogenic peptide corresponding to the hCLCA1 cleavage sequence (DABCYL-QQSGALYIPG-EDANS). Protease and substrate were incubated together for 60 min, and product formation was measured over time. Reactions were carried out in triplicate and averaged with standard deviations shown as *error bars*. Color coding is as follows: *green*, protease (10 μM) + substrate (3.25 μM); *red*, protease (10 μM) + substrate (3.25 μM) + 15 mM EDTA; *gray*, protease (10 μM) + substrate (3.25 μM) + 15 mM EDTA + 20 mM $ZnCl_2$. *E*, enzyme velocity *versus* substrate concentration plot for refolded human CLCA1 protease (22–473) (at 4 μM) using the human CLCA1 fluorogenic reporter peptide as a substrate. Three replicates were performed for each concentration. *F*, effect of commercial and custom MMP inhibitors on hCLCA1 protease activity in the fluorogenic peptide digestion assay. Reaction conditions were the same as the above with inhibitors added at 20 and 40 μM. Activity was reported as the percentage of reaction velocity in the absence of inhibitors. Reactions were carried out in triplicate. *G*, proteolysis of hCLCA1 substrate by hCLCA2 and hCLCA4 protease. Reactions are labeled as follows: *A*, substrate only; *B*, substrate + hCLCA2 protease; *C*, substrate + hCLCA4 protease. *H*, expression of a dual-tagged hCLCA1 protein in 293F cells. *Top*: schematic of the construct containing an N-terminal FLAG tag and C-terminal His_6 tag. The region containing the 8D3 mAb epitope is *highlighted*. *Bottom*: Western of supernatants from 293F cells expressing dual-tagged hCLCA1. *Left*: anti-FLAG and 8D3 mAb blot. *Right*: anti-His_6 blot. *N-term*, N terminus; *C-term*, C terminus.

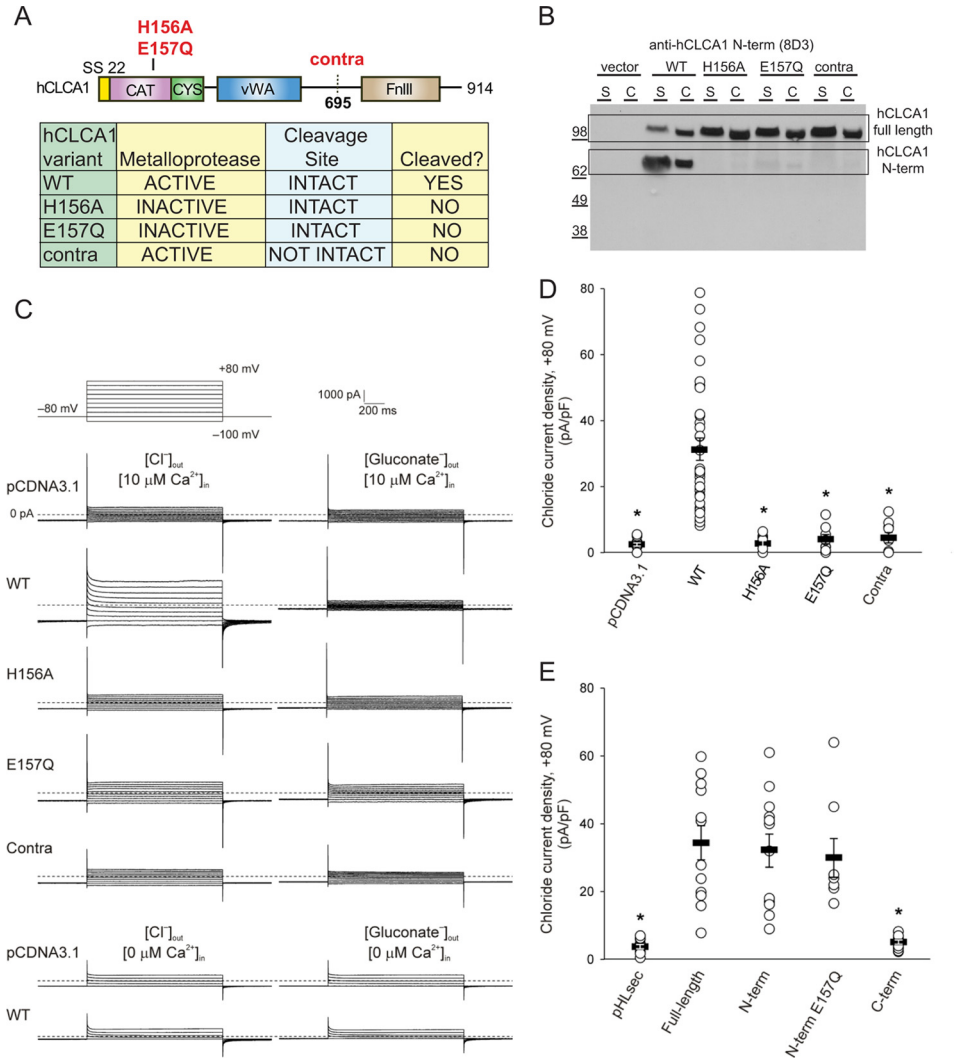

hCLCA1 variant	Metalloprotease	Cleavage Site	Cleaved?
WT	ACTIVE	INTACT	YES
H156A	INACTIVE	INTACT	NO
E157Q	INACTIVE	INTACT	NO
contra	ACTIVE	NOT INTACT	NO

FIGURE 5. **Mutations that disrupt the metalloprotease activity or the cleavage site of hCLCA1 affect Ca^{2+}-activated Cl^- currents in HEK293T cells.** *A*, schematic of hCLCA1 variants used in patch clamp electrophysiology experiments. The table summarizes the biochemical properties of each variant. Labels denote the following: *SS*, signal sequence; *CAT*, metalloprotease catalytic domain; *CYS*, Cys-rich domain; *WT*, wild type sequence; *contra*, severe mutations contrary to the CLCA consensus cleavage sequence. *B*, expression levels of hCLCA1 proteins in the same cells used for electrophysiology. *S*, supernatants; *C*, lysed cells. *C*, whole-cell currents measured in representative cells transfected with empty pCDNA3.1 plasmid, wild-type (*WT*) hCLCA1, or mutant hCLCA1, superfused with standard extracellular solution ($[Cl^-]_{out}$, *left*) and after replacement of external Cl^- with gluconate ($[Gluconate^-]_{out}$, *right*). For most experiments, the pipette solution contained 10 μM free Ca^{2+} ($[10\ \mu M\ Ca^{2+}]_{in}$), and the pulse protocol is shown at the *top left*. Selected experiments were performed in the absence of pipette Ca^{2+} ($[0\ \mu M\ Ca^{2+}]_{in}$); in those, a simplified pulse protocol was used in which the voltage was held at −80 mV and stepped from −80 mV to +80 mV in 40-mV increments. Outward currents are represented by *upward deflections*, and the *dotted lines* indicate zero current. Membrane capacitance was similar in all cases at ~25 pF. *D*, density of chloride currents at +80 mV. Values represent the difference between current density in presence (total) and absence (background) of extracellular Cl^-. *Circles* represent data from individual patches (n = 10–35); *bars* indicate the means ± S.E. of all experiments. *, $p <$ 0.001 as compared with the WT (unpaired Student's t test). *E*, Cl^- current density at +80 mV in cells transfected with empty pHLsec vector or full-length, C-terminal (*C-term*) or N-terminal (*N-term*) hCLCA1, in the absence (N-terminal) or presence of a metalloprotease-disrupting mutation (*N-term E157Q*). *Circles* represent data from individual patches (n = 7–12); *bars* indicate the means ± S.E. of all experiments. *, $p <$ 0.001 as compared with the full-length (unpaired Student's t test).

ment and unmask the N-terminal fragment for interaction with the channel.

Proteolytic Activity of the CLCA1 N-terminal Fragment Is Not Required to Modulate CaCC Currents—To address whether the proteolytic activity of the N-terminal fragment was required for activation of CaCCs, we assessed the ability of the E157Q variant of this fragment to induce Ca^{2+}-dependent currents in HEK293T cells. In cells transfected with this variant, Cl^- current density was close to that of the WT N-terminal fragment (30 ± 6 pA/pF, Fig. 5*E*). This demonstrates that gating of CaCCs by the N-terminal fragment of CLCA1 does not involve direct proteolytic clipping of the channel and suggests a direct interaction that induces gating.

DISCUSSION

CLCA1 Is a Self-cleaving Zincin Metalloprotease—Since their discovery nearly two decades ago (36), there has been much controversy regarding the specific functions of CLCA proteins and their connection to CaCC activity (9). In the present study, we demonstrate that CLCA proteins, specifically CLCA1, utilize a distinct self-processing mechanism in regulating CaCC activity. This discovery is supported by several novel findings.

First, we have demonstrated that CLCA proteins represent a novel class of zincin metalloproteases capable of self- and cross-cleavage. It should be noted that previous studies have attempted to address the issue of CLCA metalloprotease activity (28, 29); however, these studies were based on experiments utilizing CLCA proteins found in crude membrane fractions. The authors claimed that purified CLCA proteins could not be produced. Here, using purified proteins, peptides, and a comprehensive functional analysis, we unambiguously demonstrate that CLCAs are novel zincin metalloproteases that self-cleave. Up to the present study, the recognized secreted mammalian zincin endopeptidases consisted of MMP, membrane-bound MMP (MTMMP), ADAM, and ADAMTS families (26). These metalloproteases all contain a H**E***XX*H*XX*G*XX*(H/D) catalytic motif, with zinc-binding histidines (the third histidine is sometimes replaced by aspartate) and the catalytically required base/acid glutamate (bold) (27). Mutational and sequence analysis of the novel CLCA metalloprotease domain reveals a related H**E***XX*H*XXX*G*XX*DE catalytic motif. Aside from histidine, aspartate is the most common residue in the third chelating position. However, aspartate is not strictly conserved at that position within the CLCA family, whereas the adjacent (and chemically similar) glutamate is invariant (Fig. 3*C*). Mutational analysis indicates that both residues are structurally required for self-processing, although based on the current data, we cannot conclude whether the aspartate or glutamate constitutes the third zinc-binding residue. Regardless of this identity, the CLCA catalytic motif appears to be unique among secreted mammalian zincin metalloproteases.

A second key aspect of our findings relates to the regulation of metalloprotease activity. This is typically controlled at four levels: expression; compartmentalization; pro-enzyme activation; and inactivation (usually by inhibitors). MMP and ADAM proteins are secreted as zymogens that contain an N-terminal prodomain of around 80–100 amino acids, which folds against and blocks the catalytic active site (37). Removal of the prodomain is required for substrate molecules to access the active site cleft. However, a similar prodomain arrangement does not appear to be present in the CLCA proteins as the beginning of the predicted metalloprotease catalytic domain is within 10–20 residues of the N terminus of the mature protein. Furthermore, the processing of a dual-tagged CLCA1 protein indicates that an N-terminal prodomain is not present. Thus, the regulation of CLCA metalloproteases has distinct features that suggest the regulation of specific CLCA proteins will be unique and specific to their function. The observation that the addition of a TEV protease sequence into CLCA1 in the presence of TEV protease indicates that the cleavage site may be buried in the natively folded full-length protein, suggesting that regulation may be achieved by conformational change. The trigger for cleavage is uncertain, but it is possible that the shift in pH that occurs along the secretory pathway (starting from pH 7.4 in the ER to 5.5 in secretory endosomes) could control the compartmental location of cleavage. Additionally, from the current data, it is unclear whether self-cleavage predominantly occurs intra- or intermolecularly. Future studies will be required to define this mechanism and evaluate the role of endogenous metalloprotease inhibitors, such as the tissue inhibitor of metalloproteinase (TIMP) proteins (38), in the regulation of CLCA protease activity.

A third unique aspect revealed by our analysis of CLCA metalloprotease activity is the distinct nature of the consensus cleavage site in CLCA proteins. The sequence for this site shows extreme conservation on the prime (′) side of the scissile bond (Fig. 1*B*), suggesting that the substrate-binding cleft in the CLCA metalloproteases is similar in feature to others in that its specificity is mainly built into the prime side, with the unprimed side being rather flat and featureless (27). Sequence analysis of the mammalian CLCA proteins suggests the presence of a cysteine-rich domain (containing six invariant cysteines) adjacent to the catalytic domain (Fig. 3*A*). Cys-rich domains are found in a number of ADAM and ADAMTS family members; they control substrate selectivity and access to the catalytic site (26). MMP (39) and ADAM family (26, 31) proteases play key roles as modulators of inflammation and innate immunity through activation or inactivation of cytokines, chemokines, or other proteins. The major substrate of the CLCA metalloprotease domains appears to be the CLCA protein itself, but given the central involvement of CLCAs in chronic inflammatory airway diseases, additional CLCA protease substrates should also be considered.

Self-cleavage Is a Required Feature of CaCC Activation—We demonstrate that CLCA proteins are distinct in their mode of modifying ion channel activity. In particular, the observation that self-cleavage of CLCA1 is required for regulation of CaCC activity introduces a novel mechanism for controlling ion channel gating. The CLCA mechanism exhibits some similarity to the $\alpha_2\delta$ subunit of voltage-gated calcium channels, which are also secreted, proteolytically cleaved, and contain a VWA domain (40). Proteolysis cleaves this protein into two pieces and also relieves the α_2 subunit from a transmembrane domain, and these events are required for enhanced surface expression of voltage-gated calcium channels (41). However, although $\alpha_2\delta$ subunits do contain an uncharacterized N-terminal domain, they do not appear to contain features consistent with being a metalloprotease, nor do structure prediction algorithms detect the presence of one.

Our data also indicate details of a mechanism of how CLCA1, and CLCA proteins in general, activate CaCCs. It has been proposed that CLCA1 increases CaCC conductance by directly affecting the permeation pathway, rather than via enhanced trafficking or surface expression of endogenous channels (9). Our results demonstrate that proteolytic cleavage is required for CLCA1-mediated activation of CaCCs, and the N-terminal fragment alone is sufficient for activation. Additionally, the fact that the N-terminal fragment E157Q variant is able to activate CaCCs just as effectively as WT demonstrates that the proteolytic activity of this fragment is not required to activate the channel. This suggests that the CLCA1 N-terminal fragment activates CaCCs by direct interaction with the channel. This mechanism is thus distinct from the manner by which secreted proteases activate epithelial sodium channels (ENaCs) in the airway through proteolysis of the channel (42). We propose that the C-terminal fragment of CLCA masks the N-terminal region in the full-length protein and that self-cleavage is required to expose the N-terminal fragment, which can then interact with

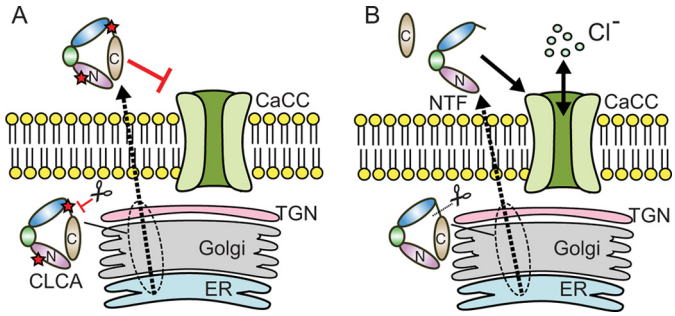

FIGURE 6. **A model of CLCA1 action based on the current data.** *A*, CLCA1 variants with inhibitory mutations in the metalloprotease domain or cleavage site (*red stars*) are produced in the secretory pathway and secreted as full-length molecules, which are unable to productively interact with a CaCC due to masking by the C-terminal portion of CLCA1. *TGN*, trans-Golgi network; *ER*, endoplasmic reticulum. *B*, native CLCA1 undergoes self-cleavage in the secretory pathway, releasing the C-terminal fragment and allowing for the N-terminal fragment (*NTF*) to engage and activate a CaCC.

the channel (Fig. 6). The precise nature of these interactions remains to be addressed.

Consequences for Airway Disease Mechanisms and Therapies—Although the precise identity of the CaCC activated by CLCAs is uncertain, a primary candidate is the anoctamin (also called TMEM16) family of proteins, which are the only presently identified CaCC proteins (43). Within this family, only Ano1 and Ano2 have been shown to be surface-expressed and create Ca^{2+}-activated Cl^- currents (44, 45). Studies in Ano1$^{-/-}$ mice indicate that Ano1-mediated Cl^- secretion is necessary for normal airway surface liquid homeostasis (46), implying a similar functional role to CFTR in the airway. Future studies will be required to determine whether this potential functional association between CLCA and anoctamin family members is based on direct physical association.

The identification of self-processing of CLCA1 as a requirement for modulation of CaCC activity has significant implications for airway disease. In CF, CLCA1 activity appears to produce improvement of the CF phenotype by activation of compensating Cl^- channels (17, 47). In asthma and chronic obstructive pulmonary disease, increased CLCA1 activity is linked to increased mucus production (16), but any connection to CaCC activity still needs to be defined. Our study is the first to provide experimental approaches aimed at dissecting these two seemingly conflicting functional roles of CLCAs by biochemically characterizing mutations that prevent CaCC activation and identifying the fragment responsible for activation. Our findings also raise the intriguing possibility of developing CLCA1 protease inhibitors as research tools and therapeutic agents. The observed differences in effectiveness among MMP-like inhibitors at blocking CLCA1 metalloprotease activity provides useful insights for the design of potent and specific CLCA1 inhibitors. The main structural difference between these inhibitors is side chain size for the predicted S2′ moiety (indole, isopropyl, phenyl, and isobutyl for GM-6001, Marimastat, Batimastat, and Zeynepstat001, respectively) (supplemental Fig. S1). Our results suggest that a larger hydrophobic residue in the S2′ pocket produces a more effective inhibitor, possibly via strengthening noncovalent interactions. These findings may be useful in guiding the design of more potent and specific CLCA metalloprotease inhibitors to prevent excess CLCA1 activity found in airway disease and perhaps cancer as well.

A final implication of our findings derives from the differences in function between human CLCA proteins. Of the three CLCA proteins expressed at mucosal surfaces (CLCA1, CLCA2, and CLCA4), only CLCA1 appears to regulate mucin gene expression and consequent mucus production (16), although CLCA1 and CLCA2 can both regulate CaCC activity (9, 48) (CLCA4 has not been tested). A thorough mechanistic understanding of how CLCA2 (or CLCA4) is able to activate CaCCs without triggering mucus production could lead to the development of novel selective CF therapeutics that exploit these mechanisms.

Acknowledgments—We thank Jen Alexander-Brett and Christopher Nelson for valuable experimental suggestions and Gregory Goldberg for valuable suggestions on the manuscript.

REFERENCES

1. Walia, V., Yu, Y., Cao, D., Sun, M., McLean, J. R., Hollier, B. G., Cheng, J., Mani, S. A., Rao, K., Premkumar, L., and Elble, R. C. (2012) Loss of breast epithelial marker hCLCA2 promotes epithelial-to-mesenchymal transition and indicates higher risk of metastasis. *Oncogene* **31,** 2237–2246
2. Walia, V., Ding, M., Kumar, S., Nie, D., Premkumar, L. S., and Elble, R. C. (2009) hCLCA2 Is a p53-inducible inhibitor of breast cancer cell proliferation. *Cancer Res.* **69,** 6624–6632
3. Patel, A. C., Brett, T. J., and Holtzman, M. J. (2009) The role of CLCA proteins in inflammatory airway disease. *Annu. Rev. Physiol.* **71,** 425–449
4. Yamazaki, J., Okamura, K., Ishibashi, K., and Kitamura, K. (2005) Characterization of CLCA protein expressed in ductal cells of rat salivary glands. *Biochim. Biophys. Acta* **1715,** 132–144
5. Loewen, M. E., and Forsyth, G. W. (2005) Structure and function of CLCA proteins. *Physiol. Rev.* **85,** 1061–1092
6. Gibson, A., Lewis, A. P., Affleck, K., Aitken, A. J., Meldrum, E., and Thompson, N. (2005) hCLCA1 and mCLCA3 are secreted non-integral membrane proteins and therefore are not ion channels. *J. Biol. Chem.* **280,** 27205–27212
7. Mundhenk, L., Alfalah, M., Elble, R. C., Pauli, B. U., Naim, H. Y., and Gruber, A. D. (2006) Both cleavage products of the mCLCA3 protein are secreted soluble proteins. *J. Biol. Chem.* **281,** 30072–30080
8. Huan, C., Greene, K. S., Shui, B., Spizz, G., Sun, H., Doran, R. M., Fisher, P. J., Roberson, M. S., Elble, R. C., and Kotlikoff, M. I. (2008) mCLCA4 ER processing and secretion requires luminal sorting motifs. *Am. J. Physiol. Cell Physiol.* **295,** C279–C287
9. Hamann, M., Gibson, A., Davies, N., Jowett, A., Walhin, J. P., Partington, L., Affleck, K., Trezise, D., and Main, M. (2009) Human ClCa1 modulates anionic conduction of calcium-dependent chloride currents. *J. Physiol.* **587,** 2255–2274
10. Kamada, F., Suzuki, Y., Shao, C., Tamari, M., Hasegawa, K., Hirota, T., Shimizu, M., Takahashi, N., Mao, X. Q., Doi, S., Fujiwara, H., Miyatake, A., Fujita, K., Chiba, Y., Aoki, Y., Kure, S., Tamura, G., Shirakawa, T., and Matsubara, Y. (2004) Association of the *hCLCA1* gene with childhood and adult asthma. *Genes Immun.* **5,** 540–547
11. Hegab, A. E., Sakamoto, T., Uchida, Y., Nomura, A., Ishii, Y., Morishima, Y., Mochizuki, M., Kimura, T., Saitoh, W., Massoud, H. H., Massoud, H. M., Hassanein, K. M., and Sekizawa, K. (2004) *CLCA1* gene polymorphisms in chronic obstructive pulmonary disease. *J. Med. Genet.* **41,** e27
12. Anton, F., Leverkoehne, I., Mundhenk, L., Thoreson, W. B., and Gruber, A. D. (2005) Overexpression of eCLCA1 in small airways of horses with recurrent airway obstruction. *J. Histochem. Cytochem.* **53,** 1011–1021
13. Nakanishi, A., Morita, S., Iwashita, H., Sagiya, Y., Ashida, Y., Shirafuji, H., Fujisawa, Y., Nishimura, O., and Fujino, M. (2001) Role of gob-5 in mucus overproduction and airway hyperresponsiveness in asthma. *Proc. Natl. Acad. Sci. U.S.A.* **98,** 5175–5180

14. Patel, A. C., Morton, J. D., Kim, E. Y., Alevy, Y., Swanson, S., Tucker, J., Huang, G., Agapov, E., Phillips, T. E., Fuentes, M. E., Iglesias, A., Aud, D., Allard, J. D., Dabbagh, K., Peltz, G., and Holtzman, M. J. (2006) Genetic segregation of airway disease traits despite redundancy of calcium-activated chloride channel family members. *Physiol. Genomics* **25,** 502–513
15. Range, F., Mundhenk, L., and Gruber, A. D. (2007) A soluble secreted glycoprotein (eCLCA1) is overexpressed due to goblet cell hyperplasia and metaplasia in horses with recurrent airway obstruction. *Vet. Pathol.* **44,** 901–911
16. Alevy, Y. G., Patel, A. C., Romero, A. G., Patel, D. A., Tucker, J., Roswit, W. T., Miller, C. A., Heier, R. F., Beyers, D. E., Brett, T. J., and Holtzman, M. J. (2012) IL-13-induced airway mucus production is attenuated by MAPK13 inhibition. *J. Clin. Invest.*, in press
17. Young, F. D., Newbigging, S., Choi, C., Keet, M., Kent, G., and Rozmahel, R. F. (2007) Amelioration of cystic fibrosis intestinal mucous disease in mice by restoration of mCLCA3. *Gastroenterology* **133,** 1928–1937
18. van der Doef, H. P., Slieker, M. G., Staab, D., Alizadeh, B. Z., Seia, M., Colombo, C., van der Ent, C. K., Nickel, R., Witt, H., and Houwen, R. H. (2010) Association of the CLCA1 p.S357N variant with meconium ileus in European patients with cystic fibrosis. *J. Pediatr. Gastroenterol. Nutr.* **50,** 347–349
19. Turk, B. (2006) Targeting proteases: successes, failures, and future prospects. *Nat. Rev. Drug Discov.* **5,** 785–799
20. Aricescu, A. R., Lu, W., and Jones, E. Y. (2006) A time- and cost-efficient system for high-level protein production in mammalian cells. *Acta Crystallogr. D Biol. Crystallogr.* **62,** 1243–1250
21. Bothe, M. K., Braun, J., Mundhenk, L., and Gruber, A. D. (2008) Murine mCLCA6 is an integral apical membrane protein of non-goblet cell enterocytes and co-localizes with the cystic fibrosis transmembrane conductance regulator. *J. Histochem. Cytochem.* **56,** 495–509
22. Braun, J., Bothe, M. K., Mundhenk, L., Beck, C. L., and Gruber, A. D. (2010) Murine mCLCA5 is expressed in granular layer keratinocytes of stratified epithelia. *Histochem. Cell Biol.* **133,** 285–299
23. Rawlings, N. D., Barrett, A. J., and Bateman, A. (2010) MEROPS: the peptidase database. *Nucleic Acids Res.* **38,** D227–D233
24. Pawłowski, K., Lepistö, M., Meinander, N., Sivars, U., Varga, M., and Wieslander, E. (2006) Novel conserved hydrolase domain in the CLCA family of alleged calcium-activated chloride channels. *Proteins* **63,** 424–439
25. Kelley, L. A., and Sternberg, M. J. (2009) Protein structure prediction on the Web: a case study using the Phyre server. *Nat. Protoc.* **4,** 363–371
26. Edwards, D. R., Handsley, M. M., and Pennington, C. J. (2008) The ADAM metalloproteinases. *Mol. Aspects Med.* **29,** 258–289
27. Tallant, C., Marrero, A., and Gomis-Rüth, F. X. (2010) Matrix metalloproteinases: fold and function of their catalytic domains. *Biochim. Biophys. Acta* **1803,** 20–28
28. Bothe, M. K., Mundhenk, L., Kaup, M., Weise, C., and Gruber, A. D. (2011) The murine goblet cell protein mCLCA3 is a zinc-dependent metalloprotease with autoproteolytic activity. *Mol. Cells* **32,** 535–541
29. Bothe, M. K., Mundhenk, L., Beck, C. L., Kaup, M., and Gruber, A. D. (2012) Impaired autoproteolytic cleavage of mCLCA6, a murine integral membrane protein expressed in enterocytes, leads to cleavage at the plasma membrane instead of the endoplasmic reticulum. *Mol. Cells* **33,** 251–257
30. Devel, L., Czarny, B., Beau, F., Georgiadis, D., Stura, E., and Dive, V. (2010) Third generation of matrix metalloprotease inhibitors: Gain in selectivity by targeting the depth of the S1′ cavity. *Biochimie* **92,** 1501–1508
31. Tortorella, M. D., Malfait, F., Barve, R. A., Shieh, H. S., and Malfait, A. M. (2009) A review of the ADAMTS family, pharmaceutical targets of the future. *Curr. Pharm. Des.* **15,** 2359–2374
32. Evans, S. R., Thoreson, W. B., and Beck, C. L. (2004) Molecular and functional analyses of two new calcium-activated chloride channel family members from mouse eye and intestine. *J. Biol. Chem.* **279,** 41792–41800
33. Jeong, S. M., Park, H. K., Yoon, I. S., Lee, J. H., Kim, J. H., Jang, C. G., Lee, C. J., and Nah, S. Y. (2005) Cloning and expression of Ca^{2+}-activated chloride channel from rat brain. *Biochem. Biophys. Res. Commun.* **334,** 569–576
34. Pifferi, S., Dibattista, M., and Menini, A. (2009) TMEM16B induces chloride currents activated by calcium in mammalian cells. *Pflugers Arch.* **458,** 1023–1038
35. Yamamura, A., Yamamura, H., Zeifman, A., and Yuan, J. X. (2011) Activity of Ca-activated Cl channels contributes to regulating receptor- and store-operated Ca entry in human pulmonary artery smooth muscle cells. *Pulm. Circ.* **1,** 269–279
36. Cunningham, S. A., Awayda, M. S., Bubien, J. K., Ismailov, I. I., Arrate, M. P., Berdiev, B. K., Benos, D. J., and Fuller, C. M. (1995) Cloning of an epithelial chloride channel from bovine trachea. *J. Biol. Chem.* **270,** 31016–31026
37. Gomis-Rüth, F. X. (2009) Catalytic domain architecture of metzincin metalloproteases. *J. Biol. Chem.* **284,** 15353–15357
38. Brew, K., and Nagase, H. (2010) The tissue inhibitors of metalloproteinases (TIMPs): an ancient family with structural and functional diversity. *Biochim. Biophys. Acta* **1803,** 55–71
39. Parks, W. C., Wilson, C. L., and López-Boado, Y. S. (2004) Matrix metalloproteinases as modulators of inflammation and innate immunity. *Nat. Rev. Immunol.* **4,** 617–629
40. Bauer, C. S., Tran-Van-Minh, A., Kadurin, I., and Dolphin, A. C. (2010) A new look at calcium channel $\alpha_2\delta$ subunits. *Curr. Opin. Neurobiol.* **20,** 563–571
41. Andrade, A., Sandoval, A., Oviedo, N., De Waard, M., Elias, D., and Felix, R. (2007) Proteolytic cleavage of the voltage-gated Ca^{2+} channel $\alpha_2\delta$ subunit: structural and functional features. *Eur. J. Neurosci.* **25,** 1705–1710
42. Kleyman, T. R., Carattino, M. D., and Hughey, R. P. (2009) ENaC at the cutting edge: regulation of epithelial sodium channels by proteases. *J. Biol. Chem.* **284,** 20447–20451
43. Galietta, L. J. (2009) The TMEM16 protein family: a new class of chloride channels? *Biophys. J.* **97,** 3047–3053
44. Duran, C., Qu, Z., Osunkoya, A. O., Cui, Y., and Hartzell, H. C. (2012) ANOs 3–7 in the anoctamin/Tmem16 Cl^- channel family are intracellular proteins. *Am. J. Physiol. Cell Physiol.* **302,** C482–493
45. Duran, C., and Hartzell, H. C. (2011) Physiological roles and diseases of Tmem16/Anoctamin proteins: are they all chloride channels? *Acta Pharmacol. Sin.* **32,** 685–692
46. Rock, J. R., O'Neal, W. K., Gabriel, S. E., Randell, S. H., Harfe, B. D., Boucher, R. C., and Grubb, B. R. (2009) Transmembrane protein 16A (TMEM16A) is a Ca^{2+}-regulated Cl^- secretory channel in mouse airways. *J. Biol. Chem.* **284,** 14875–14880
47. Ritzka, M., Stanke, F., Jansen, S., Gruber, A. D., Pusch, L., Woelfl, S., Veeze, H. J., Halley, D. J., and Tümmler, B. (2004) The *CLCA* gene locus as a modulator of the gastrointestinal basic defect in cystic fibrosis. *Hum. Genet.* **115,** 483–491
48. Gruber, A. D., Schreur, K. D., Ji, H. L., Fuller, C. M., and Pauli, B. U. (1999) Molecular cloning and transmembrane structure of hCLCA2 from human lung, trachea, and mammary gland. *Am. J. Physiol.* **276,** C1261–C1270
49. Barton, G. J. (1993) ALSCRIPT: a tool to format multiple sequence alignments. *Protein Eng.* **6,** 37–40
50. Gerhardt, S., Hassall, G., Hawtin, P., McCall, E., Flavell, L., Minshull, C., Hargreaves, D., Ting, A., Pauptit, R. A., Parker, A. E., and Abbott, W. M. (2007) Crystal structures of human ADAMTS-1 reveal a conserved catalytic domain and a disintegrin-like domain with a fold homologous to cysteine-rich domains. *J. Mol. Biol.* **373,** 891–902